

Phase diagram of the $su(8)$ quantum spin tube

J. de Gier, M. T. Batchelor and M. Maslen

*Department of Mathematics, School of Mathematical Sciences,
Australian National University, Canberra ACT 0200, Australia*

(November 12, 2018)

We calculate the phase diagram of an integrable anisotropic 3-leg quantum spin tube connected to the $su(8)$ algebra. We find several quantum phase transitions for antiferromagnetic rung couplings. Their locations are calculated exactly from the Bethe Ansatz solution and we discuss the nature of each of the different phases.

PACS: 75.10.Jm, 64.60.Cn

I. INTRODUCTION

The properties of n -leg quantum spin ladders have attracted considerable recent attention from both theorists and experimentalists [1]. The main reasons for this interest are that, like their one-dimensional counterparts, ladders are amenable to approximation schemes such as bosonization, and to accurate numerical investigation by the DMRG method. It is now well established that the n -leg Heisenberg ladders have the rather striking property of being massive for n even and massless for n odd. A number of ladder-like compounds have been found. For example, the 2-leg ladders $SrCu_2O_3$ [2] and $Cu_2(C_5H_{12}N_2)_2Cl_4$ [3] exhibit a gap, while the 3-leg ladder $Sr_2Cu_3O_5$ [2] is gapless.

Although the Heisenberg ladders are not solvable in the sense of the Heisenberg spin chain, a number of solvable ladder models are known [4–11]. One 2-leg ladder model with fixed rung, leg and diagonal interactions is equivalent to the XXZ chain at $\Delta = -\frac{5}{3}$ and is thus massive [5,6]. Another 2-leg model has been constructed which is massless in the absence of rung interactions with a transition to a massive phase at a critical (non-zero) value of the rung coupling [7]. This is in contrast with the 2-leg Heisenberg spin ladder for which the transition to the massive phase is at zero rung coupling. In the integrable model the Heisenberg rung interactions appear as chemical potentials which break the underlying $su(4)$ symmetry. The phase diagram of this model has been established by means of the Bethe Ansatz solution [7]. The integrable model has been generalised to an arbitrary number of legs in which the underlying $su(2^n)$ symmetry is broken by the Heisenberg rung interactions, which again appear as chemical potentials in the Bethe Ansatz solution [8]. Integrable ladder models with Hubbard [9] and $t - J$ [10] interactions have also been recently found. Others have been constructed with $o(2^n)$ and $sp(2^n)$ symmetry [11]. Some ladder models have also been constructed with dimer or matrix product ground states [12].

In this paper we investigate the thermodynamic properties of the solvable 3-leg quantum spin tube [8].

II. THE MODEL

We consider an integrable 3-leg spin ladder, or spin tube for periodic boundary conditions. The spins along each leg and each rung have an isotropic Heisenberg interaction, with the introduction of many-body terms to retain integrability. As usual, it is convenient to express the Hamiltonian in terms of the Pauli matrices,

$$\sigma^x = \begin{pmatrix} 0 & 1 \\ 1 & 0 \end{pmatrix}, \quad \sigma^y = \begin{pmatrix} 0 & -i \\ i & 0 \end{pmatrix}, \quad \sigma^z = \begin{pmatrix} 1 & 0 \\ 0 & -1 \end{pmatrix}. \quad (2.1)$$

The Hamiltonian of our model is

$$H = \sum_{i=1}^L h_{i,i+1}^{\text{leg}} + \sum_{i=1}^L h_i^{\text{rung}}, \quad (2.2)$$

where, taking the numbering on each elementary triangular plaquette to be ${}_2\Delta_3^1$,

$$h_{i,j}^{\text{leg}} = \frac{1}{8} \prod_{l=1}^3 \left(1 + \boldsymbol{\sigma}_i^{(l)} \cdot \boldsymbol{\sigma}_j^{(l)} \right), \quad (2.3)$$

$$h_i^{\text{rung}} = \sum_{l=1}^3 \frac{1}{2} J_l \left(\boldsymbol{\sigma}_i^{(l)} \cdot \boldsymbol{\sigma}_i^{(l+1)} - 1 \right). \quad (2.4)$$

The operators $(\sigma^x)_i^{(l)}$, $(\sigma^y)_i^{(l)}$ and $(\sigma^z)_i^{(l)}$ act as the corresponding Pauli matrices on the (i, l) th factor in the Hilbert space,

$$\mathcal{H} = \bigotimes_{i=1}^L V_i, \quad V_i = \bigotimes_{l=1}^3 C^2. \quad (2.5)$$

We take periodic boundary conditions along and also across the ladder. Now we note that $h_{i,j}^{\text{leg}}$ is just the permutator on the space $V_i \otimes V_j$ and thus that (2.3) is simply the integrable isotropic permutation Hamiltonian corresponding to the $su(8)$ algebra [13]. Since $[h_{i,j}^{\text{leg}}, h_i^{\text{rung}} + h_{i+1}^{\text{rung}}] = 0$, H defined in (2.2) is also integrable. We set $J_1 = J_2 = J$ and $J_3 = J'$, so that we can go from the isotropic tube, $J' = J$, to the ladder, $J' = 0$. This model thus generalizes that given in [8] to anisotropic rung couplings.

It is convenient to change to the basis where the square and the z -component of the total spin of a given triangle, $\mathbf{S} = \boldsymbol{\sigma}^{(1)} + \boldsymbol{\sigma}^{(2)} + \boldsymbol{\sigma}^{(3)}$ are diagonal. It follows that the eight states on a given triangle fall into a spin- $\frac{3}{2}$ quadruplet and two spin- $\frac{1}{2}$ doublets. This basis, in terms of the $(\sigma^z)^{(l)}$ eigenvalues, is,

$$\begin{aligned} |0\rangle &= |\frac{1}{2}; \frac{1}{2}\rangle_1 = \frac{1}{\sqrt{6}} \left(2 \begin{smallmatrix} + & & \\ - & + & + \\ & + & - \end{smallmatrix} - \begin{smallmatrix} + & & \\ + & + & - \\ & + & + \end{smallmatrix} - \begin{smallmatrix} - & & \\ + & + & + \\ & + & - \end{smallmatrix} \right) \\ |1\rangle &= |\frac{1}{2}; -\frac{1}{2}\rangle_1 = \frac{1}{\sqrt{6}} \left(2 \begin{smallmatrix} - & & \\ + & - & - \\ & - & + \end{smallmatrix} - \begin{smallmatrix} - & & \\ - & + & - \\ & - & + \end{smallmatrix} - \begin{smallmatrix} + & & \\ - & - & - \\ & - & + \end{smallmatrix} \right) \\ |2\rangle &= |\frac{1}{2}; \frac{1}{2}\rangle_2 = \frac{1}{\sqrt{2}} \left(\begin{smallmatrix} + & & \\ + & - & - \\ & + & + \end{smallmatrix} - \begin{smallmatrix} - & & \\ + & + & + \\ & + & - \end{smallmatrix} \right) \\ |3\rangle &= |\frac{1}{2}; -\frac{1}{2}\rangle_2 = \frac{1}{\sqrt{2}} \left(\begin{smallmatrix} - & & \\ - & + & - \\ & - & + \end{smallmatrix} - \begin{smallmatrix} + & & \\ - & - & - \\ & - & + \end{smallmatrix} \right) \\ |4\rangle &= |\frac{3}{2}; \frac{3}{2}\rangle = \begin{smallmatrix} + & & \\ + & + & + \\ & + & + \end{smallmatrix} \\ |5\rangle &= |\frac{3}{2}; \frac{1}{2}\rangle = \frac{1}{\sqrt{3}} \left(\begin{smallmatrix} - & & \\ + & + & + \\ & + & + \end{smallmatrix} + \begin{smallmatrix} + & & \\ - & + & + \\ & + & + \end{smallmatrix} + \begin{smallmatrix} + & & \\ + & - & + \\ & + & + \end{smallmatrix} \right) \\ |6\rangle &= |\frac{3}{2}; -\frac{1}{2}\rangle = \frac{1}{\sqrt{3}} \left(\begin{smallmatrix} + & & \\ - & + & + \\ & + & + \end{smallmatrix} + \begin{smallmatrix} - & & \\ + & - & + \\ & + & + \end{smallmatrix} + \begin{smallmatrix} - & & \\ - & - & + \\ & + & + \end{smallmatrix} \right) \\ |7\rangle &= |\frac{3}{2}; -\frac{3}{2}\rangle = \begin{smallmatrix} - & & \\ - & - & - \\ & - & - \end{smallmatrix} \end{aligned} \quad (2.6)$$

It is emphasized that the Hamiltonian (2.3) has the same form on this new basis. The rung Hamiltonian (2.4) now becomes diagonal and is given by $h^{\text{rung}} = \text{diag}\{-3J, -3J, -2J' - J, -2J' - J, 0, 0, 0, 0\}$.

As claimed above, H can be diagonalized using the Bethe Ansatz. The Bethe Ansatz equations are well known [13], and given by

$$\begin{aligned} \left(\frac{\lambda_j^{(1)} - \frac{i}{2}}{\lambda_j^{(1)} + \frac{i}{2}} \right)^L &= \prod_{k \neq j}^{M_1} \frac{\lambda_j^{(1)} - \lambda_k^{(1)} - i}{\lambda_j^{(1)} - \lambda_k^{(1)} + i} \prod_{k=1}^{M_2} \frac{\lambda_j^{(1)} - \lambda_k^{(2)} + \frac{i}{2}}{\lambda_j^{(1)} - \lambda_k^{(2)} - \frac{i}{2}}, \\ \prod_{k \neq j}^{M_r} \frac{\lambda_j^{(r)} - \lambda_k^{(r)} - i}{\lambda_j^{(r)} - \lambda_k^{(r)} + i} &= \prod_{k=1}^{M_{r-1}} \frac{\lambda_j^{(r)} - \lambda_k^{(r-1)} - \frac{i}{2}}{\lambda_j^{(r)} - \lambda_k^{(r-1)} + \frac{i}{2}} \prod_{k=1}^{M_{r+1}} \frac{\lambda_j^{(r)} - \lambda_k^{(r+1)} - \frac{i}{2}}{\lambda_j^{(r)} - \lambda_k^{(r+1)} + \frac{i}{2}}, \end{aligned} \quad (2.7)$$

where $j = 1, \dots, M_r$ with $r = 2, \dots, 7$ and $M_8 = 0$. The eigenenergies of $\sum_{i=1}^L h_{i,i+1}^{\text{leg}}$ are given by

$$E^{\text{leg}} = - \sum_{j=1}^{M_1} \frac{1}{(\lambda_j^{(1)})^2 + \frac{1}{4}}. \quad (2.8)$$

It is important to note that since the permutator (2.3) is invariant under any ordering of the states (2.6), this result may be obtained using any choice of reference state (or pseudo-vacuum) $|\Omega\rangle$ and any assignment of Bethe Ansatz pseudo particles. For each choice however, one has to re-interpret the numbers M_r in terms of those corresponding to the ordering chosen in (2.6). The rung Hamiltonian does alter with the choice of ordering, but the change is just a rearrangement of its eigenvalues along the diagonal. We use this property to our advantage by doing calculations with that choice of ordering for which the Bethe Ansatz reference state is closest to the true ground state of the system. Below we list the six different possibilities corresponding to the choice of ordering of the two doublets and the quadruplet.

$$1. \{|0\rangle, |1\rangle, |2\rangle, |3\rangle, |4\rangle, |5\rangle, |6\rangle, |7\rangle\}, \quad E = E^{\text{leg}} + 2(J - J')M_2 + (2J' + J)M_4.$$

The Bethe Ansatz reference state is

$$|\Omega\rangle = \bigotimes_{i=1}^L |0\rangle_i = \bigotimes_{i=1}^L |\frac{1}{2}; \frac{1}{2}\rangle_1^i,$$

and the assignment of pseudo particles is such that $M_k = \sum_{r=k}^7 N_r$, where N_r is the number of states $|r\rangle$ occurring in an excited state. In the cases below the reference state is understood to be the tensor product of the first state listed.

$$2. \{|2\rangle, |3\rangle, |0\rangle, |1\rangle, |4\rangle, |5\rangle, |6\rangle, |7\rangle\}, \quad E = E^{\text{leg}} + 2(J' - J)M_2 + 3JM_4.$$

Now the pseudo particle assignment is given by $M_1 = N_0 + N_1 + N_3 + \sum_{r=4}^7 N_r$, $M_2 = N_0 + N_1 + \sum_{r=4}^7 N_r$, $M_3 = N_1 + \sum_{r=4}^7 N_r$ and $M_k = \sum_{r=k}^7 N_r$ for $k \geq 4$.

$$3. \{|2\rangle, |3\rangle, |4\rangle, |5\rangle, |6\rangle, |7\rangle, |0\rangle, |1\rangle\}, \quad E = E^{\text{leg}} + (2J' + J)M_2 - 3JM_6,$$

with $M_k = \sum_{r=0}^1 N_r + \sum_{r=k+2}^7 N_r$ for $1 \leq k \leq 5$, $M_6 = N_0 + N_1$ and $M_7 = N_1$.

$$4. \{|4\rangle, |5\rangle, |6\rangle, |7\rangle, |2\rangle, |3\rangle, |0\rangle, |1\rangle\}, \quad E = E^{\text{leg}} - (2J' + J)M_4 + 2(J' - J)M_6,$$

with $M_k = \sum_{r=0}^3 N_r + \sum_{r=k+4}^7 N_r$ for $k \leq 3$ and $M_4 = N_0 + N_1 + N_2 + N_3$, $M_5 = N_0 + N_1 + N_3$, $M_6 = N_0 + N_1$ and $M_7 = N_1$.

$$5. \{|4\rangle, |5\rangle, |6\rangle, |7\rangle, |0\rangle, |1\rangle, |2\rangle, |3\rangle\}, \quad E = E^{\text{leg}} - 3JM_4 + 2(J - J')M_6,$$

with $M_k = \sum_{r=0}^3 N_r + \sum_{r=k+4}^7 N_r$ for $k \leq 3$ and $M_k = \sum_{r=k-4}^3 N_r$ for $k \geq 4$.

$$6. \{|0\rangle, |1\rangle, |4\rangle, |5\rangle, |6\rangle, |7\rangle, |2\rangle, |3\rangle\}, \quad E = E^{\text{leg}} + 3JM_2 - (2J' + J)M_6,$$

with $M_1 = N_1 + M_2$, $M_k = \sum_{r=2}^3 N_r + \sum_{r=k+2}^7 N_r$ for $2 \leq k \leq 5$, $M_6 = N_2 + N_3$ and $M_7 = N_3$.

Of course, all of these different choices for the reference state do not change the physics, but it turns out that each of them is convenient in some part of the phase diagram, as we will see in Section IV. Before calculating the complete phase diagram we first consider two interesting lines.

III. SPECIAL LINES

A. The tube: $J' = J$

Due to the extra symmetry in this case, the two doublets become degenerate. Consider now the Bethe Ansatz where the reference state is the spin up state of either of the spin- $\frac{1}{2}$ doublets. According to case 1. or 2. in Section II, the energy is given by

$$E = - \sum_{i=1}^{M_1} \frac{1}{(\lambda_j^{(1)})^2 + \frac{1}{4}} + 3JM_4, \quad (3.1)$$

where M_4 denotes the number of quadruplet excitations. It is obvious that if J is large and positive, no quadruplet state can exist in the ground state. There are three Fermi seas and therefore three gapless excitations. All flavours

of the quadruplet excitations are massive and their gap may be calculated by creating a $\lambda^{(4)}$ mode and a $\lambda^{(3)}$ hole in the Bethe Ansatz equation [7] (see Appendix A). The gap is

$$\Delta = 3J - \frac{1}{4}(\log 4 + \pi). \quad (3.2)$$

Thus we find a phase transition from $J > J_c^+ = \frac{1}{12}(\log 4 + \pi)$ to $0 < J < J_c^+$ where all quadruplet flavours become massless and there are seven Fermi seas and no massive excitations. Note that only at $J = 0$, all Fermi seas are completely filled.

Considering the case $J < 0$, it is convenient to choose either case 4. or 5. of Section II. The energy is given by

$$E = - \sum_{i=1}^{M_1} \frac{1}{(\lambda_j^{(1)})^2 + \frac{1}{4}} + 3|J|M_4, \quad (3.3)$$

where now M_4 denotes the number of excitations on the spin- $\frac{3}{2}$ ground state. These excitations are the four flavours belonging to the two spin- $\frac{1}{2}$ states and are all massive for $J \ll 0$. We can use the same calculation as above to conclude that again there is a phase transition at $J = J_c = -J_c^+$ where the two spin- $\frac{1}{2}$ doublet excitations become massless.

B. The ladder: $J' = 0$

As above, we start by considering this case for $J > 0$. It is most convenient to take the Bethe Ansatz as in case 1. of Section II. The energy is thus given by

$$E = - \sum_{i=1}^{M_1} \frac{1}{(\lambda_j^{(1)})^2 + \frac{1}{4}} + 2JM_2 + JM_4. \quad (3.4)$$

For $J \gg 0$ it is obvious that $M_2 = 0$ for the ground state. The ground state is thus formed by the $\{|0\rangle, |1\rangle\}$ doublet and there is one gapless excitation and six massive ones. As before we can calculate the gap by introducing a $\lambda^{(2)}$ mode and a $\lambda^{(1)}$ hole, giving rise to

$$\Delta = 2J - 2 \int_0^\infty \frac{e^{-\omega}}{1 + e^{-\omega}} d\omega = 2(J - \log 2). \quad (3.5)$$

This gap thus closes at $J_{c,1} = \log 2$ and for $J < J_{c,1}$ there are three massless excitations and four massive ones corresponding to the triplet states. These become massless at a second critical point, $J_{c,2}$, whose value can not be calculated analytically. This point continuously connects to the critical point J_c^+ on the line $J' = J$.

IV. PHASES

As already noted, the different choices of the reference state do not change the physics, but each of them is convenient in some part of the phase diagram. To appreciate this, it is helpful to divide the phase diagram into six regions defined by the lines $J = 0$, $J' = J$ and $2J' + J = 0$ as in Fig. 1. In each of these regions, the corresponding choice of reference state of Section II is the most convenient.

1. $J > 0$, $J - J' > 0$ and $2J' + J > 0$.

This part of the phase diagram contains the ladder for $J > 0$. As in Section III B we choose to describe the spectrum as in case 1. of the list in Section II. For $J \gg J'$ it is obvious that for the ground state one must have $M_2 = 0$. The ground state thus is formed by the doublet $\{|0\rangle, |1\rangle\}$, which is effectively a spin- $\frac{1}{2}$ XXX chain. The system is critical with one massless excitation and six massive ones. The gap can again be calculated by creating a $\lambda^{(2)}$ mode and a $\lambda^{(1)}$ hole ($M_2 \rightarrow 1$, $M_1 \rightarrow M_1 - 1$) in the Bethe Ansatz equations, and is given by

$$\Delta = 2(J - J') - 2 \log 2. \quad (4.1)$$

Thus there is a critical line on which this gap vanishes, given by

$$J'_c = J - \log 2. \quad (4.2)$$

Above this line some of the excitations on the $\{|0\rangle, |1\rangle\}$ doublet become massless. We now investigate which ones. From the form of the energy it follows that if $2J' + J$ is large, $M_4 = 0$ and only the $\{|2\rangle, |3\rangle\}$ doublet excitations have become massless. Thus for large $2J' + J$ and above the critical line (4.2), the ground state is given by the two spin- $\frac{1}{2}$ doublets and the quadruplet excitations are massive. There is another phase transition where also the quadruplet excitations become massless, i.e. $M_4 \neq 0$ for the ground state, and its location on the line (4.2) is given by

$$2J'_c + J = 0, \quad \text{or} \quad (J, J') = \left(\frac{2}{3} \log 2, -\frac{1}{3} \log 2\right). \quad (4.3)$$

Its location changes as M_2 increases, which can be calculated using perturbative calculations (see Appendix B). It ultimately reaches the value of

$$(J, J') = \left(\frac{1}{12}(\log 4 + \pi), \frac{1}{12}(\log 4 + \pi)\right), \quad (4.4)$$

on the line $J' = J$ where three Fermi seas are completely filled instead of just one.

2. $J > 0, J - J' < 0$ and $2J' + J > 0$.

By the same reasoning as above the ground state is again formed by a doublet for $J' \gg J$, but now $\{|2\rangle, |3\rangle\}$ since we use a different reference state. The system again is critical with one massless excitation and six massive ones. The gap can be calculated similarly and the critical line on which this gap vanishes is given by

$$J'_c = J + \log 2. \quad (4.5)$$

Below this line the $\{|0\rangle, |1\rangle\}$ doublet excitations have become massless. There is another phase transition where also the quadruplet excitations become massless, i.e. $M_4 \neq 0$ for the ground state, and its location on the line (4.5) is given by

$$(J, J') = (0, \log 2). \quad (4.6)$$

Its location changes as M_2 increases reaching the previously calculated value,

$$(J, J') = \left(\frac{1}{12}(\log 4 + \pi), \frac{1}{12}(\log 4 + \pi)\right), \quad (4.7)$$

on the line $J' = J$ where three Fermi seas are completely filled instead of just one.

3. $J < 0, J - J' < 0$ and $2J' + J > 0$.

Here we find the phase boundary,

$$2J'_c + J = 2 \log 2, \quad (4.8)$$

where the spin- $\frac{3}{2}$ quadruplet excitations on the $\{|2\rangle, |3\rangle\}$ doublet ground state become massless. The point on this line where also the spin- $\frac{1}{2}$ doublet $\{|0\rangle, |1\rangle\}$ becomes massless is given by

$$J = 0. \quad (4.9)$$

As before, its location changes, reaching

$$(J, J') = \left(-\frac{\alpha_6}{3}, \frac{\alpha_6}{6}\right), \quad \alpha_6 \approx 0.5076..., \quad (4.10)$$

on the line $2J' + J = 0$.

4. $J < 0$, $J - J' < 0$ and $2J' + J < 0$.

In this region the ground state for large and negative $2J' + J$ is the quadruplet. It's smallest excitations, those of the $\{|2\rangle, |3\rangle\}$ doublet, become massless at

$$2J' + J = -\frac{1}{4}(\pi + \log 4). \quad (4.11)$$

On this line the other doublet becomes massless at

$$(J, J') = \left(-\frac{1}{12}(\pi + \log 4), -\frac{1}{12}(\pi + \log 4)\right), \quad (4.12)$$

on the line $J' = J$. This point moves to

$$(J, J') = \left(-\frac{\alpha_6}{3}, \frac{\alpha_6}{6}\right), \quad (4.13)$$

on the line $2J' + J = 0$.

5. $J < 0$, $J - J' > 0$ and $2J' + J < 0$.

In this region the quadruplet is still the ground state for large J , but now the lowest excitations are the $\{|0\rangle, |1\rangle\}$ doublet. They become massless at

$$J = -\frac{1}{12}(\pi + \log 4), \quad (4.14)$$

independent of J' . The other doublet becomes massless at

$$(J, J') = \left(-\frac{1}{12}(\pi + \log 4), -\frac{1}{12}(\pi + \log 4)\right), \quad (4.15)$$

on the line $J' = J$ and this point extends to

$$(J, J') = \left(0, -\frac{\alpha_6}{2}\right), \quad (4.16)$$

on the line $J = 0$.

6. $J > 0$, $J - J' > 0$ and $2J' + J < 0$.

Here, the ground state for large J is the $\{|0\rangle, |1\rangle\}$ doublet, and the smallest excitations are the quadruplet which become massless at

$$J = \frac{2}{3} \log 2, \quad (4.17)$$

independent of J' . The other, doublet, excitations become massless at

$$(J, J') = \left(\frac{2}{3} \log 2, -\frac{1}{3} \log 2\right), \quad (4.18)$$

on the line $2J' + J = 0$. On the other phase boundary, $J = 0$, this point is

$$(J, J') = \left(0, -\frac{\alpha_6}{2}\right). \quad (4.19)$$

Our findings, along with the phase boundaries, are summarized in Fig. 1.

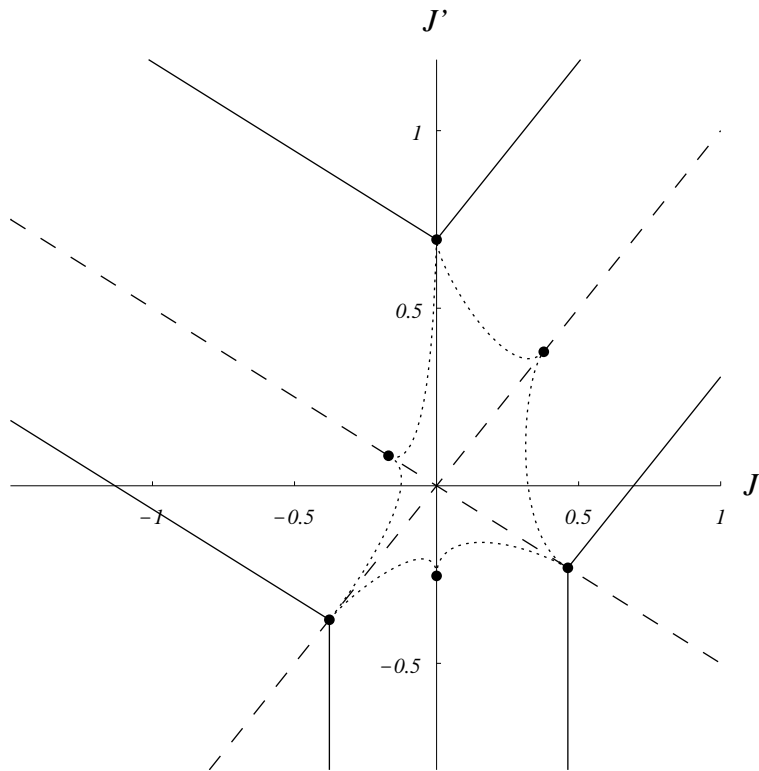


FIG. 1. Phase diagram. The dashed lines are $J' = J$ and $2J' + J = 0$ which together with the y-axis divide phase space into six regions. The dotted lines are sketches of phase boundaries.

V. CONCLUSION

In this paper we have calculated the phase diagram of the integrable anisotropic 3-leg quantum spin tube defined in (2.2). The model differs from the usual Heisenberg spin ladder in that it includes additional four- and six-body terms in the leg Hamiltonian (2.3). The phase diagram, as calculated from the Bethe Ansatz solution, is given in Fig. 1. The straight line phase boundaries can be calculated exactly as well as the critical points on the lines where the rung Hamiltonian becomes partially degenerate. For the location of the dotted phase boundaries one has to resort to perturbative calculations which show that they end parallel to the degeneracy lines. In Fig. 1 we have sketched the full form of these phase boundaries. It is to be hoped that their precise location may be accurately determined numerically.

Since the model has an odd number of legs, it is critical in the entire phase space and has no true gap. It is however the simplest example with more than one quantum phase transition for $J > 0$ and serves as an example for what to expect for higher leg ladders. In general, if the rung Hamiltonian has n different eigenvalues, one may expect $n - 1$ different phase transitions along a generic line between the phase with the lowest and highest total spin. At each of these one expects to find quantum critical behaviour, which will however diminish in magnitude.

The 3-leg quantum spin tube is also integrable in the presence of a magnetic field. The corresponding 3-leg Heisenberg model has been shown to exhibit magnetization plateaus by means of renormalization group calculations based on the bosonized effective continuum theory [14]. The exact calculation of the magnetic behaviour of the present model will thus be of considerable interest.

ACKNOWLEDGMENTS

This work has been supported by the Australian Research Council.

APPENDIX A: GAP CALCULATION

As is well known, the Bethe Ansatz equations (2.8) may be written as integral equations in the thermodynamic limit ($L \rightarrow \infty$),

$$a_1(\lambda) = \rho^{(1)}(\lambda) + \int_{-\lambda_F^{(1)}}^{\lambda_F^{(1)}} a_2(\lambda - \lambda') \rho^{(1)}(\lambda') d\lambda' - \int_{-\lambda_F^{(2)}}^{\lambda_F^{(2)}} a_1(\lambda - \lambda') \rho^{(2)}(\lambda') d\lambda', \quad (\text{A1})$$

$$\begin{aligned} \rho^{(r)}(\lambda) + \int_{-\lambda_F^{(r)}}^{\lambda_F^{(r)}} a_2(\lambda - \lambda') \rho^{(r)}(\lambda') d\lambda' = \\ \int_{-\lambda_F^{(r-1)}}^{\lambda_F^{(r-1)}} a_1(\lambda - \lambda') \rho^{(r-1)}(\lambda') d\lambda' + \int_{-\lambda_F^{(r+1)}}^{\lambda_F^{(r+1)}} a_1(\lambda - \lambda') \rho^{(r+1)}(\lambda') d\lambda', \end{aligned} \quad (\text{A2})$$

where $\rho^{(r)}$ are the distributions of Bethe Ansatz roots and holes and

$$a_n(\lambda) = \frac{n}{2\pi} \frac{1}{\lambda^2 + (\frac{n}{2})^2}. \quad (\text{A3})$$

In the sequel we will make use of the following convention for the Fourier transform,

$$\hat{f}(\omega) = \frac{1}{2\pi} \int_{-\infty}^{\infty} f(k) e^{-ik\omega} dk, \quad f(k) = \int_{-\infty}^{\infty} \hat{f}(\omega) e^{ik\omega} d\omega, \quad (\text{A4})$$

and of the results,

$$\int_{-\infty}^{\infty} a_n(k) e^{-ik\omega} dk = e^{-\frac{n}{2}|\omega|}, \quad \text{for } n > 0, \quad (\text{A5})$$

$$\int_0^{\infty} \frac{e^{-a\omega}}{1 + e^{-\omega}} d\omega = \frac{1}{2} \left(\psi^{(0)}(\frac{a+1}{2}) - \psi^{(0)}(\frac{a}{2}) \right), \quad \psi^{(0)}(z) = \frac{\Gamma'(z)}{\Gamma(z)}. \quad (\text{A6})$$

As an example we give here the calculation of the gap for the tube when $J' = J > 0$. The ground state for $J \gg 0$ consists of three completely filled Fermi seas. The Bethe Ansatz equations (A1) and (A2) may therefore be solved with Fourier transforms. A quadruplet excitation is created with a $\lambda^{(4)}$ mode and a $\lambda^{(3)}$ hole. Following Wang [7], we will denote the changes in the distribution functions as a consequence of this particle-hole pair creation by $\delta\rho^{(r)}$. The Fourier transformed Bethe Ansatz equations then become (with some abuse of notation)

$$\begin{aligned} 0 &= \delta\hat{\rho}^{(1)}(\omega)(1 + e^{-|\omega|}) - \delta\hat{\rho}^{(2)}(\omega)e^{-\frac{1}{2}|\omega|} \\ \delta\hat{\rho}^{(2)}(\omega)(1 + e^{-|\omega|}) &= \delta\hat{\rho}^{(1)}(\omega)e^{-\frac{1}{2}|\omega|} + \delta\hat{\rho}^{(3)}(\omega)e^{-\frac{1}{2}|\omega|} - \frac{1}{2\pi L} e^{-i\lambda^{(3)}\omega - \frac{1}{2}|\omega|} \\ \delta\hat{\rho}^{(3)}(\omega)(1 + e^{-|\omega|}) &= \frac{1}{2\pi L} e^{-i\lambda^{(3)}\omega - |\omega|} + \delta\hat{\rho}^{(2)}(\omega)e^{-\frac{1}{2}|\omega|} + \frac{1}{2\pi L} e^{-i\lambda^{(4)}\omega - \frac{1}{2}|\omega|}, \end{aligned}$$

from which we obtain

$$\delta\hat{\rho}^{(1)}(\omega) = \frac{1}{2\pi L} \frac{e^{-i\lambda^{(4)}\omega} - e^{\frac{1}{2}|\omega| - i\lambda^{(3)}\omega}}{4 \cosh \omega \cosh \frac{\omega}{2}}. \quad (\text{A7})$$

Thus it follows that the smallest gap ($\lambda^{(3)} \rightarrow \infty, \lambda^{(4)} \rightarrow 0$) is equal to

$$\Delta = 3J - 2\pi L \int_{-\infty}^{\infty} e^{-\frac{1}{2}|\omega|} \delta\hat{\rho}^{(1)}(\omega) d\omega = 3J - \frac{1}{4}(\log 4 + \pi). \quad (\text{A8})$$

APPENDIX B: PERTURBATIVE CALCULATIONS

Suppose we are in region I in the phase where both doublet excitations are massless, but close to the phase boundary $J' = J - \log 2$. The $\{|2\rangle, |3\rangle\}$ excitations have just become massless and M_2/L and M_3/L have a small but finite value. The $\lambda^{(2)}$ Fermi sea will be filled up to some finite momentum Λ while those of $\lambda^{(1)}$ and $\lambda^{(3)}$ are completely filled. By creating a $\lambda^{(4)}$ excitation, we change Λ and the distribution functions. The Bethe Ansatz equations for this situation are given by

$$\rho^{(1)}(\lambda) + \int_{-\infty}^{+\infty} a_2(\lambda - \lambda') \rho^{(1)}(\lambda') d\lambda' = a_1(\lambda) + \int_{-\tilde{\Lambda}}^{+\tilde{\Lambda}} a_1(\lambda - \lambda') \rho^{(2)}(\lambda') d\lambda', \quad (B1)$$

$$\rho^{(2)}(\lambda) + \int_{-\tilde{\Lambda}}^{+\tilde{\Lambda}} a_2(\lambda - \lambda') \rho^{(2)}(\lambda') d\lambda' = \int_{-\infty}^{+\infty} a_1(\lambda - \lambda') \rho^{(1)}(\lambda') d\lambda' + \int_{-\infty}^{+\infty} a_1(\lambda - \lambda') \rho^{(3)}(\lambda') d\lambda', \quad (B2)$$

$$\rho^{(3)}(\lambda) + \int_{-\infty}^{+\infty} a_2(\lambda - \lambda') \rho^{(3)}(\lambda') d\lambda' = \int_{-\tilde{\Lambda}}^{+\tilde{\Lambda}} a_1(\lambda - \lambda') \rho^{(2)}(\lambda') d\lambda' + \frac{a_1(\lambda)}{L}, \quad (B3)$$

with the conditions

$$\int_{-\tilde{\Lambda}}^{+\tilde{\Lambda}} \rho^{(2)}(\lambda) d\lambda = \frac{M_2}{L}, \quad \int_{-\infty}^{+\infty} \rho^{(3)}(\lambda) d\lambda = \frac{M_3}{L}. \quad (B4)$$

These equations can be solved perturbatively in $\tilde{\Lambda}$ which we will do up to $O(\tilde{\Lambda}^3)$. With the help of

$$\begin{aligned} \int_{-\tilde{\Lambda}}^{+\tilde{\Lambda}} a_n(\lambda - \lambda') \rho^{(2)}(\lambda') d\lambda' &= 2\tilde{\Lambda} a_n(\lambda) \rho^{(2)}(0) + \frac{1}{3} \tilde{\Lambda}^3 (a_n''(\lambda) \rho^{(2)}(0) + a_n(\lambda) \rho^{(2)''}(0)), \\ &= a_n(\lambda) \frac{M_2}{L} + \frac{1}{3} \tilde{\Lambda}^3 a_n''(\lambda) \rho^{(2)}(0), \end{aligned} \quad (B5)$$

we find

$$\hat{\rho}^{(1)}(\omega) = \frac{1}{2\pi} \frac{1}{2 \cosh \frac{\omega}{2}} \left(1 + \frac{M_2}{L} - \frac{\log 2}{3\pi} \tilde{\Lambda}^3 \omega^2 \left(1 + \frac{1}{L} \right) \right), \quad (B6)$$

$$\rho^{(2)}(0) = \frac{\log 2}{\pi} \left(1 + \frac{1}{L} \right) + O(\tilde{\Lambda}). \quad (B7)$$

Since we want to keep M_2 constant it follows from (B7) that

$$\tilde{\Lambda} = \Lambda \left(1 - \frac{1}{L} \right) + O\left(\frac{1}{L^2}\right). \quad (B8)$$

Finally, the energy is given by

$$\begin{aligned} E &= -2\pi L \int_{-\infty}^{+\infty} \hat{\rho}^{(1)}(\omega) e^{-\frac{1}{2}|\omega|} d\omega + 2(J - J')M_2 + 2J' + J \\ &= -2L \log 2 \left(1 + \frac{M_2}{L} \right) + L \tilde{\Lambda}^3 \frac{\zeta(3) \log 2}{\pi} \left(1 + \frac{1}{L} \right) + 2(J - J')M_2 + 2J' + J \\ &= -2L \log 2 - 2M_2 \left[\log 2 - \frac{1}{4}\zeta(3)\Lambda^2 - J + J' \right] + 2J' + J - \Lambda^3 \zeta(3) \frac{\log 2}{\pi} + O\left(\frac{1}{L}\right). \end{aligned} \quad (B9)$$

It thus follows that the Fermi momentum Λ is defined by

$$J' = J - \log 2 + \frac{1}{4}\zeta(3)\Lambda^2, \quad (B10)$$

and that the $\lambda^{(4)}$ become massless on this line at the point

$$2J' + J = \Lambda^3 \zeta(3) \frac{\log 2}{\pi}. \quad (B11)$$

We thus conclude that this phase boundary ends in the point

$$(J, J') = \left(\frac{2}{3} \log 2, -\frac{1}{3} \log 2 \right) \quad (\text{B12})$$

parallel to the line $2J' + J = 0$.

- [1] See, e.g., E. Dagotto and T. M. Rice, *Science* **271** 618; E. Dagotto, cond-mat/9908250, and references therein.
- [2] M. Azuma et al., *Phys. Rev. Lett.* **73**, 3463 (1994).
- [3] G. Chaboussant et al., *Phys. Rev. B* **55**, 3046 (1997).
- [4] H. Frahm and C. Rödenbeck, *Europhys. Lett.* **33**, 47 (1996); *J. Phys. A* **30**, 4467 (1997).
- [5] S. Albeverio, S.-M. Fei and Y. Wang, *Europhys. Lett.* **47**, 364 (1999).
- [6] M. T. Batchelor and M. Maslen, cond-mat/9907480.
- [7] Y. Wang, *Phys. Rev. B* **60**, 9236 (1999).
- [8] M. T. Batchelor and M. Maslen, *J. Phys. A* **32**, L377 (1999).
- [9] H. Fan, cond-mat/9908028.
- [10] H. Frahm and A. Kundu, cond-mat/9910104.
- [11] M. T. Batchelor, J. de Gier, J. Links and M. Maslen, cond-mat/9911043.
- [12] See, e.g., A.K. Kolezhuk and H.-J. Mikeska, *Int. J. Mod. Phys. B* **12**, 2325 (1998), and references therein.
- [13] B. Sutherland, *Phys. Rev. B* **12**, 3795 (1975).
- [14] R. Citro, E. Orignac, N. Andrei, C. Itoi and S. Qin, cond-mat/9904371.